

Provenance of Chinese Loess: Evidence from Stable Lead Isotope

Feng Wu^{1,*}, Steven Sai Hang Ho^{1,2}, Qianli Sun³, and Simon Ho Sai Ip²

¹State Key Laboratory of Loess and Quaternary Geology, Institute of Earth Environment, Chinese Academy of Sciences, Shaanxi, China

²Hong Kong Premium Services and Research Laboratory, Hong Kong, China

³State Key Laboratory for Estuarine and Coastal Research, East China Normal University, Shanghai, China

Received 30 August 2010, accepted 19 November 2010

ABSTRACT

Twenty-seven samples of typical loess and paleosol strata collected in nine different regions of the Chinese Loess Plateau (CLP) were fractionated into PM_{1.0}, PM_{2.5}, PM₁₀ and Total Suspended Particulates (TSP) (particulate matter with aerodynamic diameters less than 1.0, 2.5, 10 and ~30 μm, respectively) by a resuspension chamber at the Desert Research Institute (DRI; Reno, NV, United States). The amounts and isotope ratios of lead (Pb) were quantified in the loess samples. Our size-segregated analysis demonstrated that the Pb isotopic composition in the loess-paleosol deposits was preserved after grain-size sorting and that therefore the isotope ratio can serve as a proxy for source tracing. A similar pattern of Pb isotope ratios was observed for sediment collected from potential source regions and the loess samples suggested that the Gobi and deserts in southern Mongolia and northern China are major sources for the deposits in the CLP. No significant deviation of Pb isotope amount was found between the nine samples of loess and paleosol strata, implying the stability of loess sources during the glacial and interglacial regime.

Key words: Stable lead isotope, Size fractions, Provenance, Chinese Loess Plateau

Citation: Wu, F., S. S. H. Ho, Q. Sun, and S. H. S. Ip, 2011: Provenance of Chinese Loess: Evidence from stable lead isotope. *Terr. Atmos. Ocean. Sci.*, 22, 305-314, doi: 10.3319/TAO.2010.11.19.01(TT)

1. INTRODUCTION

Loess is recognized as an important paleoclimate archive, presenting a terrestrial equivalent to the deep-sea oxygen isotope record of Quaternary glacial-interglacial cycles (Porter 2001). The loess-paleosol sequence in the Chinese Loess Plateau (CLP) has long been documented as a continuous history of dust activity over 2.4 Ma (Liu 1985; An et al. 1991). Due to its eolian origin, the loess in the CLP is one of a few direct records of paleowinds that not only aid greatly in reconstructing synoptic-scale paleoclimatology (Porter and An 1995), but also provide climate information on the dust-generated area (Sun and An 2002).

The upwind regions, such as the Gobi (stony desert) and sand deserts in the northern and northwestern China are commonly regarded as potential loess sources to the CLP (Liu 1985). However, large divergences regarding the specific origins of the loess have recently been reported.

For instance, previous studies suggested that the loess is a highly mixed material from the Gobi and other deserts near the CLP and inland basins in northern and northwestern China (Gallet et al. 1996; Jahn 2001); however, Zhang et al. (1997) claimed that it originated from several source regions, e.g., western deserts (mainly the Taklamakan Desert) and northern low- and high-dust deserts (such as the Badain Juran and Tengger deserts). Comparisons between isotopes, elements and mineral compositions of fine fractions of the loess in the CLP showed that the Gobi in south Mongolia and the adjoining Gobi and sand deserts (e.g., the Badain Jaran Desert, Tengger Desert, Ulan Buh Desert, Hobq Desert and Mu Us Desert), rather than the three inland basins (including Tarim, Tsaidam and Jungar), are the major loess source regions (Sun 2002). In addition, strontium (Sr) and neodymium (Nd) isotopes in fine fractions of the Chinese loess also indicated that the north edge of Tibet (e.g., the Tsaidam Basin, the Badain Juran and Tengger deserts) is the source region which mainly contributed to the loess in the

* Corresponding author
E-mail: kurt_wf@ieecas.cn

CLP (Chen et al. 2007). Based on the results of electron spin resonance signal intensity analysis and crystallinity index (CI) measured from fine-grained quartz, Sun et al. (2008) suggested that both the Gobi desert in southern Mongolia and the sandy deserts in northern China (primarily the Badain Juran and Tengger deserts) are the major sources of eolian loess in the CLP during the last glacial-interglacial cycle.

Even though there were no significant variation of the sources reported during the deposition of loess and paleosol in the CLP (Gallet 1996; Jahn 2001), Zhang (1997) pointed out that the sources of Chinese loess varied between the north and the west source regions during the glacial and interglacial regimes. Sun (2008) further revealed a transition of the loess sources from the Gobi desert in southern Mongolia during the glacial period to the sandy desert in northern China during the interglacial regime. Such discrepancies have instigated a series of intensive researches to obtain a full understanding of the provenance of loess in the CLP as well as their climatic and environmental implications.

Lead (Pb) isotopic composition is a powerful tool for source identification because both minerals and rocks have distinct Pb isotope ratios, subject to their geological derivations. In addition, the Pb isotope ratios would not be affected, to a measurable extent, by physical or chemical fractionation processes (Bollhöfer and Rosman 2000, 2001; Veysseyre et al. 2001). Application of Pb isotopes as tracers has been successfully differentiated silt sources for the late Wisconsin loess in the central Great Plains of eastern Colorado (Aleinikoff et al. 1999). Comparisons of Pb isotopic composition of Chinese loess with the ice core and marine sediments also assisted establishment of linkage between the provenance of those sediments and the Asian inland regions (Biscaye et al. 1997; Jones et al. 2000; Pettke et al. 2000; Godfrey 2002; Stancin et al. 2006; Klemm et al. 2007). In addition, the Pb isotopic ratios have been recently demonstrated the relationship of the provenance changes (Sun and Zhu 2010).

However, loess is derived from protoliths, of which the geochemical characteristics are size-dependent. Since loess was transported by winds of different strength or underwent different transport distances in geological times, its geochemical characteristics may be changed by grain-size sorting. Previous studies on the provenance of loess using Pb isotopes focused mainly on bulk samples, and therefore no data about the distribution of Pb isotopic compositions among different size fractions of Chinese loess could be referenced. No one knows whether there is any systematic change in the source area which would be indicated by variations in wind strength or distance to the source or wind direction.

In this study, samples were collected in nine loess and paleosol strata at the Xi Feng Loess Profile. The Pb isotopes in different size fractions of loess were precisely quantified.

The objectives of this paper are to: 1) evaluate impacts of grain-size sorting on Pb isotopic compositions; and 2) track potential source regions of loess over the CLP with the Pb isotopic ratios.

2. EXPERIMENT METHODS

The CLP is one of the most extensive areas of loess deposition in the world. It spans an area of approximately 440000 km², predominantly in the provinces of Shanxi, Shaanxi and Gasnu, between 33 - 40°N and 98 - 115°E (Liu 1985) (Fig. 1). Xi Feng (35°45'N, 107°49'E), a city of Shaanxi province, is located in the central CLP. Its profile contains more than 30 loess-paleosol layers and represents an exceptionally long record of the Asian dust deposits for 2.5 Ma. Loess samples were taken from nine representative loess and paleosol horizons, which are respectively named as S0, L1LL1, L1LL2, S1, L2, S2, S5, L9, and L15. Three parallel samples (~2 kg) were collected in each horizon. The loess samples were sieved through Tyler 30, 50, 100, 200, and 400 mesh sieves to obtain ca. 5 g of materials for resuspension.

The sieved loess samples were re-suspended in a chamber facility at the Desert Research Institute (DRI) at Reno, NV, United States. The experimental procedures are described in detail elsewhere (Chow et al. 1994). In the re-suspension chamber, the loess were fractionated into four sizes, including PM_{1.0}, PM_{2.5}, PM₁₀ and Total Suspended Particulates (TSP) (particulate matter with aerodynamic diameters less than 1.0, 2.5, 10 and ~30 μm, respectively), and collected onto 47 mm Teflon-membrane filters (2 mm pore size, Pall Sciences, Ann Arbor, MI, USA).

Amounts of Pb isotopes in the re-suspended samples were measured. The analytical procedures were described as follows. A whole filter sample was cut into pieces and transferred to a clean digestion tube. Fifty microliters of ethanol plus 4 ml of a 1 : 1 nitrite acid (HNO₃) and water (in volume ratio) were added into the tube. The sample was gradually digested in an oven at 95°C for 65 minutes. After cooling down to room temperature, the digestion solution was brought up to 30 ml with water. Reagent blanks and control samples were prepared in the same way. The Pb isotopes were quantified using an inductively coupled plasma-mass spectrometer (ICP-MS, X Series, Thermo Elemental). Two thallium isotopes (²⁰³Tl and ²⁰⁵Tl) were used as internal standards (IS) to correct for any instrumental drift. A digested NIST SRM 981 (Common Lead Isotopic Standard) was run per 10 samples in order to demonstrate the stability of the instrument. The Pb isotopic ratio (Pb Ratio_{corr}) was corrected by the following equation:

$$\text{Pb Ratio}_{\text{corr}} = \text{Pb Ratio}_{\text{meas}} \times (\text{NIST}_{\text{cert}} / \text{NIST}_{\text{meas}}) \quad (1)$$

where Pb Ratio_{meas} is the measured ratio in the filter sample,

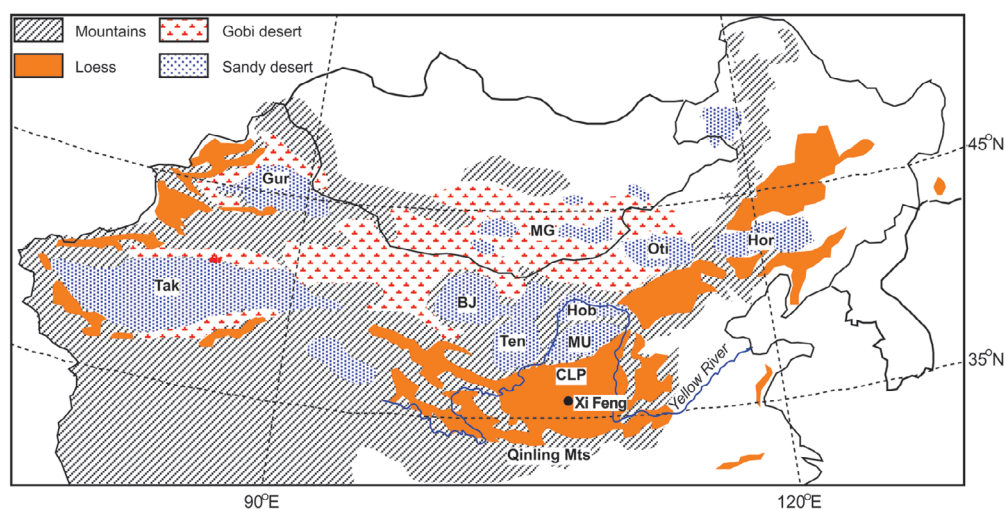


Fig. 1. Map showing the location of the Chinese Loess Plateau (CLP), the loess sampling location (black dot, Xi Feng), and the potential source regions (major Gobi, deserts, sand-land), which include the Taklimakan (Tak) desert in western China, the Badain Juran (BJ) and Tengger (Ten) deserts in northern China, and the Gobi desert in southern Mongolia (MG), Gurbantunggut desert (Gur), Mu Us desert (MU), Hobq desert (Hob), Otindag sand-land (Oti), Horqin sand-land (Hor) (Redrawn after: Sun et al. 2008).

$NIST_{cert}$ is the certificated ratio of the NIST SRM 981 sample, and $NIST_{meas}$ is the measured ratio in the NIST SRM 981 sample. Analytical uncertainty (σ_R) of the Pb ratio was calculated by adding in quadrature the uncertainties of the measured Pb ratio for the filter sample and the NIST SRM 981 sample as specified in Bevington (1969) with the equation of:

$$\sigma_R = [(\sigma S_m^2 \times N_c^2 / N_m^2) + (\sigma N_m^2 \times N_c^2 \times S_m^2 / N_m^4)]^{0.5} \quad (2)$$

where σS_m and σN_m are the standard deviation of the measured Pb ratio for a sample and the NIST SRM sample, respectively; N_c is the certified Pb ratio for the NIST SRM sample; S_m is the measured Pb ratio for a sample; and N_m is the measured Pb ratio for the NIST SRM sample.

3. RESULTS AND DISCUSSION

3.1 Impact of Grain-Size Sorting on Pb Isotopic Composition

Table 1 shows the Pb isotope ratios for $PM_{1.0}$, $PM_{2.5}$, PM_{10} and TSP in the loess samples. Good consistence was found for the ratios among three radiogenic isotopes ^{206}Pb , ^{207}Pb and ^{208}Pb in the same strata, while large variations were seen for $^{206}Pb/^{204}Pb$, $^{207}Pb/^{204}Pb$ and $^{208}Pb/^{204}Pb$. This could be explained by the limits on analytical precision of ^{204}Pb owing to its low natural abundance (Walder and Furuta 1993). Herein, ratios among three radiogenic isotopes ^{206}Pb , ^{207}Pb and ^{208}Pb will be discussed.

Mean $^{207}Pb/^{206}Pb$ and $^{208}Pb/^{206}Pb$ ratios of the four particle-size fractions in the nine strata are shown in Fig. 2. The experimental uncertainties were calculated on the basis of values from the three parallel samples collected in the same

strata. The uncertainties for $^{207}Pb/^{206}Pb$ and $^{208}Pb/^{206}Pb$ were 0.05 and 0.03, respectively. Small variations were seen for the Pb isotope ratios among the four particle-size fractions. With a difference less than < 0.0005 , average $^{207}Pb/^{206}Pb$ ratios for $PM_{1.0}$, $PM_{2.5}$, PM_{10} and TSP samples were 0.8373, 0.8374, 0.8372 and 0.8377, respectively. The largest variation of $^{207}Pb/^{206}Pb$ (0.02) and $^{208}Pb/^{206}Pb$ (0.013) occurred in the samples collected at L2 and L9, respectively. But of noted, all these variations were within the range of experimental uncertainties and thus are eligible.

Loess is a product of rock weathering; its coarse and fine fractions represent the minerals of different origins. Among them, the coarse fractions are composed mainly of primary minerals, while fine fractions are the mixtures of secondary minerals formed during chemical weathering. Since the Pb isotope ratios would not be affected, to a measurable extent, by physical or chemical fractionation processes (Bollhöfer and Rosman 2000, 2001; Veyseyre et al. 2001), the primary minerals and secondary minerals of loess should have similar lead isotope composition, which cause the similarities of lead isotopes among different size fractions. Therefore, the lead isotope composition of loess reflects the characteristics of materials in its source regions, and they can be used as potential provenance tracers of loess.

3.2 Dominant Sources of Loess and Their Glacial-Interglacial Fluctuations

The Pb isotopic compositions in the loess collected in the nine strata of the CLP are compared with eolian sand samples from the source regions in order to identify the dominant sources of loess (Fig. 3). Since the Pb isotopic compositions for eolian sand samples in the source regions

Table 1. Pb isotope ratios for PM_{1.0}, PM_{2.5}, PM₁₀ and TSP in the loess samples.

Strata	Samples ID	Size fractions	²⁰⁶ Pb/ ²⁰⁴ Pb	²⁰⁷ Pb/ ²⁰⁴ Pb	²⁰⁸ Pb/ ²⁰⁴ Pb	²⁰⁷ Pb/ ²⁰⁶ Pb	²⁰⁸ Pb/ ²⁰⁶ Pb
S0	CJZ-S0-6	TSP	18.464 ± 0.034	15.556 ± 0.037	38.376 ± 0.022	0.843 ± 0.037	2.078 ± 0.023
		PM ₁₀	18.245 ± 0.040	15.230 ± 0.044	37.709 ± 0.027	0.835 ± 0.044	2.067 ± 0.028
		PM _{2.5}	18.299 ± 0.044	15.402 ± 0.049	38.181 ± 0.031	0.842 ± 0.049	2.086 ± 0.032
		PM _{1.0}	18.603 ± 0.031	15.645 ± 0.039	38.482 ± 0.024	0.841 ± 0.039	2.069 ± 0.025
	CJZ-S0-7	TSP	18.495 ± 0.035	15.429 ± 0.041	38.512 ± 0.023	0.834 ± 0.041	2.082 ± 0.023
		PM ₁₀	18.303 ± 0.039	15.207 ± 0.042	37.884 ± 0.026	0.831 ± 0.042	2.070 ± 0.026
		PM _{2.5}	18.249 ± 0.037	15.323 ± 0.049	37.928 ± 0.029	0.840 ± 0.049	2.078 ± 0.030
		PM _{1.0}	18.927 ± 0.030	15.888 ± 0.029	39.366 ± 0.019	0.839 ± 0.029	2.080 ± 0.019
	CJZ-S0-8	TSP	18.592 ± 0.037	15.635 ± 0.035	38.603 ± 0.023	0.841 ± 0.035	2.076 ± 0.023
		PM ₁₀	18.533 ± 0.041	15.573 ± 0.046	38.673 ± 0.027	0.840 ± 0.046	2.087 ± 0.027
		PM _{2.5}	18.708 ± 0.028	15.745 ± 0.038	38.942 ± 0.019	0.842 ± 0.038	2.082 ± 0.019
		PM _{1.0}	18.491 ± 0.038	15.504 ± 0.042	38.497 ± 0.028	0.839 ± 0.042	2.082 ± 0.028
L1L1	CJZ-L1-0	TSP	18.457 ± 0.031	15.349 ± 0.040	38.300 ± 0.024	0.832 ± 0.040	2.075 ± 0.024
		PM ₁₀	18.293 ± 0.035	15.453 ± 0.043	38.106 ± 0.025	0.845 ± 0.043	2.083 ± 0.025
		PM _{2.5}	18.519 ± 0.044	15.417 ± 0.049	38.361 ± 0.031	0.833 ± 0.049	2.071 ± 0.031
		PM _{1.0}	18.712 ± 0.045	15.653 ± 0.052	38.818 ± 0.033	0.837 ± 0.052	2.075 ± 0.033
	CJZ-L1-1	TSP	18.474 ± 0.026	15.544 ± 0.031	38.315 ± 0.019	0.841 ± 0.031	2.074 ± 0.020
		PM ₁₀	18.673 ± 0.028	15.618 ± 0.037	38.680 ± 0.020	0.836 ± 0.037	2.071 ± 0.020
		PM _{2.5}	18.787 ± 0.049	15.624 ± 0.054	38.770 ± 0.034	0.832 ± 0.054	2.064 ± 0.034
		PM _{1.0}	18.780 ± 0.040	15.626 ± 0.041	38.731 ± 0.028	0.832 ± 0.041	2.062 ± 0.029
	CJZ-L1-2	TSP	18.620 ± 0.020	15.680 ± 0.030	38.787 ± 0.019	0.842 ± 0.030	2.083 ± 0.019
		PM ₁₀	18.460 ± 0.034	15.460 ± 0.037	38.406 ± 0.022	0.838 ± 0.037	2.081 ± 0.022
		PM _{2.5}	18.337 ± 0.043	15.397 ± 0.048	37.899 ± 0.033	0.840 ± 0.048	2.067 ± 0.033
		PM _{1.0}	18.833 ± 0.038	15.715 ± 0.046	38.973 ± 0.028	0.834 ± 0.046	2.069 ± 0.028
L1L2	CJZ-L1-34	TSP	18.402 ± 0.031	15.553 ± 0.035	38.285 ± 0.020	0.845 ± 0.035	2.081 ± 0.021
		PM ₁₀	18.495 ± 0.029	15.586 ± 0.030	38.346 ± 0.020	0.843 ± 0.030	2.073 ± 0.020
		PM _{2.5}	18.945 ± 0.027	15.960 ± 0.029	39.350 ± 0.018	0.842 ± 0.029	2.077 ± 0.018
		PM _{1.0}	18.491 ± 0.021	15.573 ± 0.028	38.588 ± 0.016	0.842 ± 0.028	2.087 ± 0.016
	CJZ-L1-35	PM ₁₀	18.115 ± 0.045	15.306 ± 0.048	37.709 ± 0.030	0.845 ± 0.048	2.082 ± 0.030
		PM _{2.5}	18.222 ± 0.037	15.302 ± 0.039	37.723 ± 0.025	0.840 ± 0.039	2.070 ± 0.026
		PM _{1.0}	18.610 ± 0.039	15.615 ± 0.047	38.603 ± 0.028	0.839 ± 0.047	2.074 ± 0.029
	CJZ-L1-36	TSP	18.374 ± 0.043	15.458 ± 0.053	38.106 ± 0.033	0.841 ± 0.053	2.074 ± 0.034
		PM ₁₀	18.638 ± 0.025	15.514 ± 0.026	38.361 ± 0.019	0.832 ± 0.026	2.058 ± 0.020
		PM _{2.5}	18.502 ± 0.024	15.470 ± 0.029	38.285 ± 0.019	0.836 ± 0.029	2.069 ± 0.019
		PM _{1.0}	18.283 ± 0.023	15.321 ± 0.027	37.796 ± 0.021	0.838 ± 0.027	2.067 ± 0.021

Table 1. (Continued)

Strata	Samples ID	Size fractions	$^{206}\text{Pb}/^{204}\text{Pb}$	$^{207}\text{Pb}/^{204}\text{Pb}$	$^{208}\text{Pb}/^{204}\text{Pb}$	$^{207}\text{Pb}/^{206}\text{Pb}$	$^{208}\text{Pb}/^{206}\text{Pb}$
S1	CJZ-S1-14	TSP	18.368 ± 0.030	15.517 ± 0.031	38.225 ± 0.019	0.845 ± 0.031	2.081 ± 0.019
		PM ₁₀	18.390 ± 0.030	15.605 ± 0.039	38.296 ± 0.024	0.849 ± 0.039	2.083 ± 0.024
		PM _{2.5}	18.477 ± 0.042	15.509 ± 0.042	38.285 ± 0.028	0.839 ± 0.042	2.072 ± 0.028
		PM _{1.0}	18.412 ± 0.044	15.492 ± 0.043	38.225 ± 0.027	0.841 ± 0.043	2.076 ± 0.027
	CJZ-S1-18	TSP	18.571 ± 0.034	15.588 ± 0.037	38.542 ± 0.025	0.839 ± 0.037	2.075 ± 0.025
		PM ₁₀	18.575 ± 0.041	15.663 ± 0.043	38.741 ± 0.031	0.843 ± 0.043	2.086 ± 0.031
		PM _{2.5}	18.457 ± 0.039	15.465 ± 0.041	38.391 ± 0.026	0.838 ± 0.041	2.080 ± 0.026
		PM _{1.0}	18.550 ± 0.039	15.561 ± 0.044	38.436 ± 0.026	0.839 ± 0.044	2.072 ± 0.026
	CJZ-S1-29	TSP	18.350 ± 0.041	15.436 ± 0.049	38.361 ± 0.030	0.841 ± 0.049	2.090 ± 0.031
		PM ₁₀	18.299 ± 0.037	15.240 ± 0.046	37.549 ± 0.028	0.833 ± 0.046	2.052 ± 0.028
		PM _{2.5}	18.491 ± 0.039	15.524 ± 0.039	38.361 ± 0.023	0.840 ± 0.039	2.075 ± 0.023
		PM _{1.0}	18.610 ± 0.034	15.576 ± 0.031	38.285 ± 0.024	0.837 ± 0.031	2.057 ± 0.024
L2	CJZ-L2-5	TSP	18.333 ± 0.048	15.309 ± 0.055	37.651 ± 0.034	0.835 ± 0.055	2.054 ± 0.035
		PM ₁₀	18.477 ± 0.040	15.526 ± 0.044	38.436 ± 0.027	0.840 ± 0.045	2.080 ± 0.028
		PM _{2.5}	18.436 ± 0.041	15.495 ± 0.042	38.270 ± 0.027	0.840 ± 0.042	2.076 ± 0.028
		PM _{1.0}	18.719 ± 0.035	15.738 ± 0.038	38.865 ± 0.022	0.841 ± 0.038	2.076 ± 0.022
	CJZ-L2-6	TSP	18.659 ± 0.038	15.509 ± 0.039	38.391 ± 0.028	0.831 ± 0.039	2.058 ± 0.028
		PM ₁₀	18.471 ± 0.038	15.492 ± 0.040	38.062 ± 0.025	0.839 ± 0.040	2.061 ± 0.025
		PM _{2.5}	18.780 ± 0.045	15.758 ± 0.048	38.927 ± 0.031	0.839 ± 0.048	2.073 ± 0.031
		PM _{1.0}	18.279 ± 0.037	15.359 ± 0.052	37.767 ± 0.030	0.840 ± 0.052	2.066 ± 0.030
	CJZ-L2-8	TSP	NA	NA	NA	NA	NA
		PM ₁₀	19.022 ± 0.042	15.906 ± 0.042	39.606 ± 0.027	0.836 ± 0.042	2.082 ± 0.027
		PM _{2.5}	18.543 ± 0.031	15.728 ± 0.032	38.787 ± 0.020	0.848 ± 0.032	2.092 ± 0.020
		PM _{1.0}	18.691 ± 0.039	15.653 ± 0.041	38.634 ± 0.026	0.837 ± 0.042	2.067 ± 0.026
S2	CJZ-S2-5	TSP	18.780 ± 0.037	15.590 ± 0.037	38.542 ± 0.023	0.830 ± 0.037	2.052 ± 0.023
		PM ₁₀	18.596 ± 0.028	15.630 ± 0.029	38.772 ± 0.018	0.841 ± 0.029	2.085 ± 0.019
		PM _{2.5}	18.938 ± 0.027	15.748 ± 0.022	39.051 ± 0.017	0.832 ± 0.022	2.062 ± 0.017
		PM _{1.0}	18.909 ± 0.033	15.857 ± 0.030	39.414 ± 0.022	0.839 ± 0.030	2.084 ± 0.022
	CJZ-S2-8	TSP	18.472 ± 0.048	15.415 ± 0.051	38.160 ± 0.033	0.835 ± 0.051	2.066 ± 0.033
		PM ₁₀	18.440 ± 0.034	15.512 ± 0.036	38.315 ± 0.022	0.841 ± 0.036	2.078 ± 0.023
		PM _{2.5}	18.440 ± 0.035	15.366 ± 0.041	38.076 ± 0.024	0.833 ± 0.041	2.065 ± 0.024
		PM _{1.0}	18.502 ± 0.043	15.453 ± 0.050	38.346 ± 0.027	0.835 ± 0.050	2.073 ± 0.027
	CJZ-S2-11	TSP	18.468 ± 0.038	15.603 ± 0.043	38.460 ± 0.026	0.845 ± 0.043	2.083 ± 0.027
		PM ₁₀	18.279 ± 0.023	15.376 ± 0.031	38.121 ± 0.019	0.841 ± 0.031	2.086 ± 0.019
		PM _{2.5}	18.790 ± 0.026	15.723 ± 0.028	39.004 ± 0.022	0.837 ± 0.028	2.076 ± 0.022
		PM _{1.0}	18.415 ± 0.046	15.456 ± 0.052	38.166 ± 0.034	0.839 ± 0.052	2.073 ± 0.035

Table 1. (Continued)

Strata	Samples ID	Size fractions	$^{206}\text{Pb}/^{204}\text{Pb}$	$^{207}\text{Pb}/^{204}\text{Pb}$	$^{208}\text{Pb}/^{204}\text{Pb}$	$^{207}\text{Pb}/^{206}\text{Pb}$	$^{208}\text{Pb}/^{206}\text{Pb}$
S5	CJZ-S5-I	TSP	18.866 ± 0.028	15.730 ± 0.026	38.880 ± 0.017	0.834 ± 0.026	2.061 ± 0.017
		PM ₁₀	18.869 ± 0.031	15.760 ± 0.032	39.004 ± 0.023	0.835 ± 0.032	2.067 ± 0.024
		PM _{2.5}	18.719 ± 0.031	15.608 ± 0.034	38.741 ± 0.022	0.834 ± 0.034	2.070 ± 0.023
		PM _{1.0}	18.471 ± 0.029	15.422 ± 0.031	38.136 ± 0.021	0.835 ± 0.031	2.065 ± 0.021
	CJZ-S5-II	TSP	18.659 ± 0.036	15.558 ± 0.040	38.710 ± 0.023	0.834 ± 0.040	2.075 ± 0.024
		PM ₁₀	18.684 ± 0.028	15.581 ± 0.028	38.818 ± 0.017	0.834 ± 0.028	2.078 ± 0.017
		PM _{2.5}	18.733 ± 0.023	15.695 ± 0.032	38.880 ± 0.020	0.838 ± 0.032	2.076 ± 0.020
		PM _{1.0}	18.730 ± 0.036	15.638 ± 0.040	38.849 ± 0.024	0.835 ± 0.040	2.074 ± 0.024
	CJZ-S5-III	TSP	NA	NA	NA	NA	NA
		PM ₁₀	18.495 ± 0.026	15.460 ± 0.032	38.166 ± 0.017	0.836 ± 0.032	2.064 ± 0.018
		PM _{2.5}	18.780 ± 0.035	15.665 ± 0.035	38.958 ± 0.020	0.834 ± 0.035	2.075 ± 0.020
		PM _{1.0}	18.794 ± 0.041	15.771 ± 0.051	38.803 ± 0.033	0.839 ± 0.051	2.065 ± 0.033
L9	CJZ-L9-I	TSP	18.840 ± 0.032	15.670 ± 0.030	38.757 ± 0.022	0.832 ± 0.030	2.057 ± 0.022
		PM ₁₀	18.974 ± 0.035	15.733 ± 0.042	38.911 ± 0.025	0.829 ± 0.043	2.051 ± 0.026
		PM _{2.5}	18.971 ± 0.034	15.867 ± 0.035	38.911 ± 0.024	0.836 ± 0.035	2.051 ± 0.024
		PM _{1.0}	18.557 ± 0.046	15.475 ± 0.047	38.210 ± 0.031	0.834 ± 0.047	2.059 ± 0.031
	CJZ-L9-II	TSP	18.851 ± 0.040	15.740 ± 0.040	39.145 ± 0.026	0.835 ± 0.040	2.077 ± 0.026
		PM ₁₀	18.895 ± 0.029	15.776 ± 0.032	39.114 ± 0.020	0.835 ± 0.032	2.070 ± 0.020
		PM _{2.5}	18.412 ± 0.032	15.390 ± 0.033	38.136 ± 0.022	0.836 ± 0.033	2.071 ± 0.023
		PM _{1.0}	18.808 ± 0.029	15.685 ± 0.030	39.082 ± 0.023	0.834 ± 0.030	2.078 ± 0.023
	CJZ-L9-III	TSP	18.719 ± 0.028	15.653 ± 0.031	38.726 ± 0.021	0.836 ± 0.031	2.069 ± 0.021
		PM ₁₀	18.855 ± 0.024	15.645 ± 0.030	38.927 ± 0.020	0.830 ± 0.030	2.065 ± 0.020
		PM _{2.5}	18.712 ± 0.044	15.643 ± 0.048	38.695 ± 0.031	0.836 ± 0.048	2.068 ± 0.031
		PM _{1.0}	18.659 ± 0.045	15.487 ± 0.049	38.436 ± 0.031	0.830 ± 0.049	2.060 ± 0.032
L15	CJZ-L15-I	TSP	18.464 ± 0.037	15.504 ± 0.040	38.285 ± 0.024	0.840 ± 0.040	2.074 ± 0.025
		PM ₁₀	18.740 ± 0.032	15.546 ± 0.038	38.649 ± 0.025	0.830 ± 0.038	2.062 ± 0.025
		PM _{2.5}	18.613 ± 0.028	15.581 ± 0.035	38.482 ± 0.017	0.837 ± 0.035	2.067 ± 0.018
		PM _{1.0}	18.744 ± 0.047	15.693 ± 0.052	38.787 ± 0.031	0.837 ± 0.052	2.069 ± 0.032
	CJZ-L15-II	TSP	18.610 ± 0.037	15.670 ± 0.044	38.512 ± 0.027	0.842 ± 0.044	2.070 ± 0.028
		PM ₁₀	18.564 ± 0.033	15.434 ± 0.034	38.315 ± 0.020	0.831 ± 0.034	2.064 ± 0.021
		PM _{2.5}	18.751 ± 0.036	15.655 ± 0.045	38.818 ± 0.027	0.835 ± 0.045	2.070 ± 0.028
		PM _{1.0}	18.491 ± 0.037	15.558 ± 0.040	38.391 ± 0.027	0.841 ± 0.040	2.076 ± 0.027
	CJZ-L15-III	TSP	18.931 ± 0.040	15.776 ± 0.042	39.114 ± 0.026	0.833 ± 0.042	2.066 ± 0.027
		PM ₁₀	18.634 ± 0.048	15.613 ± 0.053	38.421 ± 0.032	0.838 ± 0.053	2.062 ± 0.033
		PM _{2.5}	18.540 ± 0.034	15.458 ± 0.031	38.376 ± 0.020	0.834 ± 0.031	2.070 ± 0.021
		PM _{1.0}	18.391 ± 0.050	15.313 ± 0.060	37.855 ± 0.035	0.833 ± 0.060	2.058 ± 0.035

Note: NA = not analyzed.

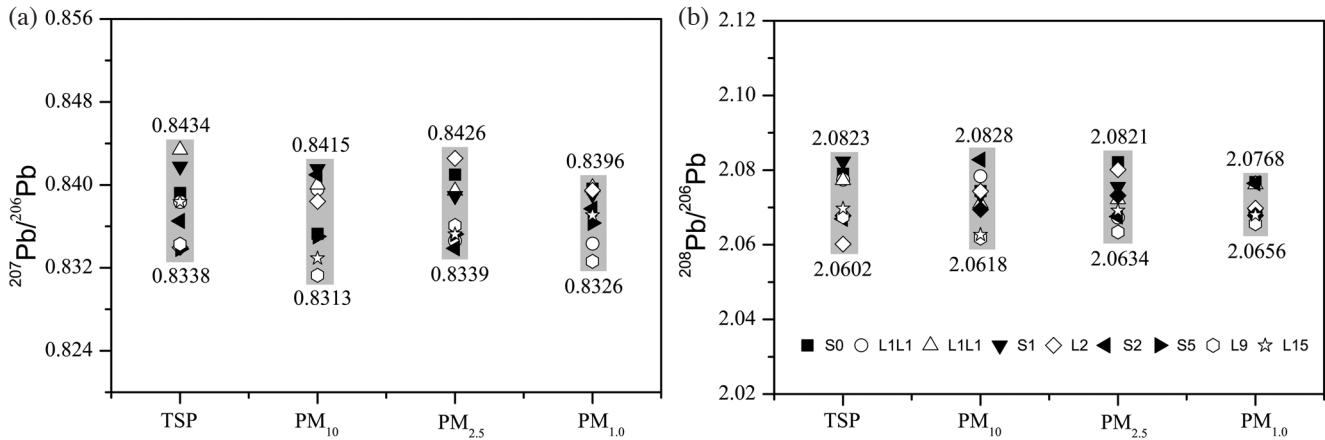


Fig. 2. $^{207}\text{Pb}/^{206}\text{Pb}$ (a) and $^{208}\text{Pb}/^{206}\text{Pb}$ (b) for $\text{PM}_{1.0}$, $\text{PM}_{2.5}$, PM_{10} and TSP of the nine loess and paleosol strata. The maximum and minimum values of $^{207}\text{Pb}/^{206}\text{Pb}$ and $^{208}\text{Pb}/^{206}\text{Pb}$ are labeled.

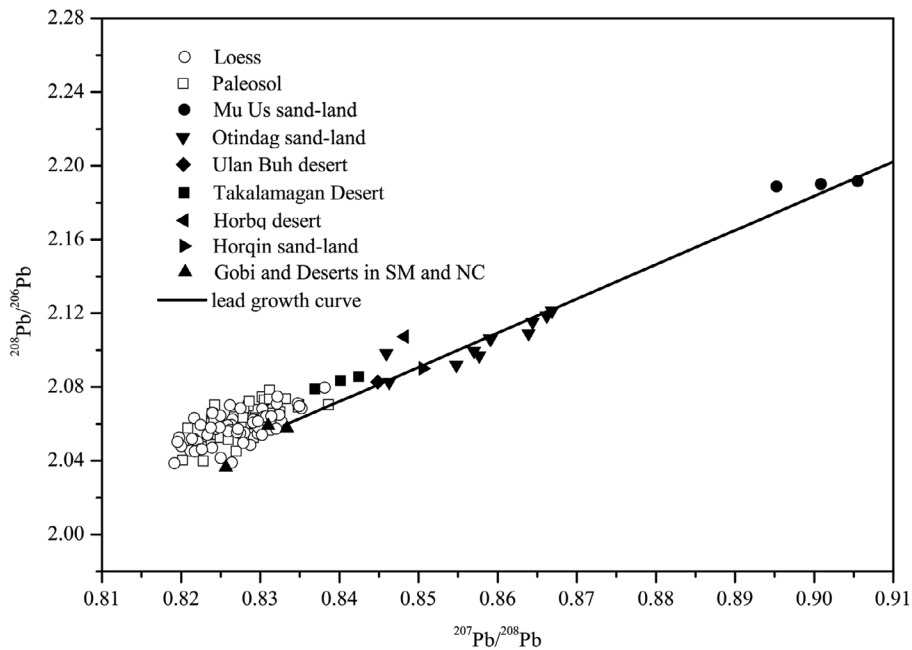


Fig. 3. Pb isotopic ratios plot ($^{207}\text{Pb}/^{206}\text{Pb}$ vs. $^{208}\text{Pb}/^{206}\text{Pb}$) in Chinese loess and desert dust from different source areas. The data for eolian sand samples of Takalamagan Desert, Mu Us Deserts, Ulan Buh Desert, Hobq Desert, Otindag Daka and Horqin sand-land are from Li (2007); and the data of Tengger Deserts and the Gobi Desert in southern Mongolia (SM) and north China (NC) are from Bicaye et al. (1997). The growth curve of Pb ore in north China are plotted based on the data of Zhu (1995).

are generally for their silicate fraction, we discuss first the difference of lead isotope ratios between bulk samples and silicate fractions of loess. Table 2 compares the Pb isotopic compositions for bulk samples and silicate fractions of eight loess samples, which were analyzed at the same time by Jones et al. (2000). It can be seen that the Pb isotopic compositions of loess were systematically lower in the silicate fractions than in the bulk samples. All these data were translated into those of the silicate fraction by subtracting a factor of 0.010 and 0.012 for $^{207}\text{Pb}/^{206}\text{Pb}$ and $^{208}\text{Pb}/^{206}\text{Pb}$, respectively.

As a successful source tracer of loess, the Pb isotopic ratios in sediments from different source regions can be distinguished. Analysis of Pb isotopes in the eolian sand samples of the potential source regions, including the Takalamagan Desert, Mu Us Desert, Ulan Buh Desert, Hobq Desert, Otindag sand-land, Horqin sand-land, Tengger Deserts, and the Gobi in southern Mongolia, have shown that the Pb isotopic ratios were consequently varied (Bicaye 1997; Li 2007). Based on the Pb isotopic compositions, four major source regions were identified: 1) the west source regions as represented by the Taklamakan desert; 2) the Mu Us

Table 2. Differences of $^{207}\text{Pb}/^{206}\text{Pb}$ and $^{208}\text{Pb}/^{206}\text{Pb}$ between bulk loess and the extracted silicate fraction.

Sample	$^{207}\text{Pb}/^{206}\text{Pb}$			$^{208}\text{Pb}/^{206}\text{Pb}$		
	Bulk	Sil	Difference	Bulk	Sil	Difference
LS6	0.834	0.824	0.010	2.076	2.063	0.012
LS9	0.834	0.827	0.007	2.074	2.068	0.007
LS14	0.833	0.823	0.010	2.074	2.065	0.009
LS18	0.834	0.823	0.011	2.077	2.060	0.017
LS22	0.834	0.822	0.012	2.075	2.060	0.015
LS27	0.834	0.822	0.012	2.077	2.060	0.017
LS30	0.834	0.829	0.005	2.075	2.074	0.001
LS33	0.834	0.820	0.013	2.076	2.057	0.018
Average			0.010			0.012

Note: All data are from Jones et al. (2001); Bulk = bulk loess; Sil = extracted silicate fraction.

deserts; 3) the Gobi and deserts in southern Mongolia and northern China; and 4) the Hobq, and Ulan Buh deserts and the sand-lands in northeastern China.

The $^{207}\text{Pb}/^{206}\text{Pb}$ and $^{208}\text{Pb}/^{206}\text{Pb}$ ratios of the eolian sand in the Mu Us Desert were 50% and 60% higher than those of the loess in the CLP. They are two completely different end-members and located at opposite ends of the Pb isotope growth line. Our results obviously indicate that the Mu Us Desert is unlikely to be the major source contributing region to the loess deposited in the CLP. In addition, the $^{207}\text{Pb}/^{206}\text{Pb}$ and $^{208}\text{Pb}/^{206}\text{Pb}$ ratios of the Hobq Desert, the Ulan Buh Desert and the sand-land in northeastern China had a 30% and 40% higher than those of the loess in the CLP. In fact, the dusts from the Hobq and Ulan Buh Deserts are very limited, and the Otindag and Horqin sand-lands are not located in an upwind position of the CLP. Both of them are thus unexpected as the potential sources of Chinese loess (Sun et al. 2008). The two Pb isotopic compositions of the loess were much close to those of eolian sand in the Taklamagan Desert (with an increase of 10%). Unfortunately, we cannot determine lower Pb isotope ratios in any samples collected in all potential source regions. As a result, no solid conclusion can be drawn regarding whether these regional sources were fully- or partially-dominated in the contributions of the CLP.

Conversely, the Pb isotopic compositions of the loess in the CLP, in fact, fell in the range of the Gobi and deserts in southern Mongolia and northern China, thus possibly representing the main source regions of the Chinese loess. Our conclusion is consistent with the findings from Sun (2002) that the Gobi in southern Mongolia and the adjoining Gobi and sand deserts (including the Badain Jaran Desert, Tengger Desert, Ulan Buh Desert, Hobq Desert and Mu Us Desert), rather than the inland basins, are the dominant source

areas of the CLP. Further, Sun et al. (2008) support our finding that the fine-grained dust deposits on the CLP originate mainly from the Gobi desert in southern Mongolia and the sandy deserts in northern China (primarily the Badain Jaran and Tengger deserts), rather than from the Taklimakan desert in western China, at least during the last climatic cycle. Chen et al. (2007) reported the Nd-Sr isotopic compositions of the loess. Their results also suggest that the main source regions of the last glacial loess in the CLP are the Badain Jaran Desert, Tengger Desert, and Qaidam Desert, even though the Qaidam Desert region is not covered in our study.

Vertical variations of Pb isotopic ratios in different horizons can also be seen in Fig. 2. Only small deviations between the loess and paleosol samples were found. In the TSP fraction, the highest amounts of $^{207}\text{Pb}/^{206}\text{Pb}$ (0.8434) and $^{208}\text{Pb}/^{206}\text{Pb}$ (2.0823) were seen in the samples of L1L1 and S1, respectively, while the lowest were in S5 (0.8338) and L2 (2.0602), respectively. The differences of maximum to minimum values were again below the experimental uncertainties. This implies that the dominant source regions of the loess in the CLP were relatively stable and had no significant variations during the glacial and interglacial regime.

4. SUMMARY

The grain-size impact on the Pb isotopic composition of loess in the central CLP is insignificant, and therefore our result suggest that a Pb isotopic composition can be used as a proxy for source tracing. The comparisons of Pb isotopic compositions between loess and eolian sand in the arid and semi-arid regions in the northern and northwestern China evidenced that the Gobi and deserts in southern Mongolia and northern China are the main source regions of loess in

the CLP. No obvious deviations of Pb isotopes were obtained between the nine horizontal layers in the loess and paleosol samples, implying the loess source regions were stable during the glacial and interglacial regime.

Acknowledgements This work was supported by grant from the Chinese National Science Foundation (40872211; 40599424). The authors are grateful to Prof. Judith C. Chow and John G. Watson of the Desert Research Institute (DRI, Reno, NV, United States) for their assistance in the sample analysis. We are also extremely grateful to Prof. Youbin Sun of IEECAS for his suggestion regarding to the interpretation of Pb isotopic ratios plot.

REFERENCES

- Aleinikoff, J. N., D. R. Muhs, R. R. Sauer, and C. M. Faning, 1999: Late Quaternary loess in northeastern Colorado: Part II - Pb isotopic evidence for the variability of loess sources. *Geol. Soc. Am. Bull.*, **111**, 1876-1883, doi: 10.1130/0016-7606(1999)111<1876:LQLINC>2.3.CO;2. [\[Link\]](#)
- An, Z., G. Kukla, S. C. Porter, and J. Xiao, 1991: Late Quaternary dust flow on the Chinese Loess Plateau. *Catena*, **18**, 125-132, doi: 10.1016/0341-8162(91)90012-M. [\[Link\]](#)
- Bevington, P. R., 1969: Data Reduction and Error Analysis for the Physical Sciences. McGraw Hill, New York, NY.
- Biscaye, P. E., F. E. Grousset, M. Revel, S. VanderGaast, G. A. Zielinski, A. Vaars, and G. Kukla, 1997: Asian provenance of glacial dust (stage 2) in the Greenland Ice Sheet Project 2 Ice Core, Summit, Greenland. *J. Geophys. Res.*, **102**, 26765-26780, doi: 10.1029/97JC01249. [\[Link\]](#)
- Bollhöfer, A. and K. J. R. Rosman, 2000: Isotopic source signatures for atmospheric lead: The Southern Hemisphere. *Geochim. Cosmochim. Acta*, **64**, 3251-3262, doi: 10.1016/S0016-7037(00)00436-1. [\[Link\]](#)
- Bollhöfer, A. and K. J. R. Rosman, 2001: Isotopic source signatures for atmospheric lead: The Northern Hemisphere. *Geochim. Cosmochim. Acta*, **65**, 1727-1740, doi: 10.1016/S0016-7037(00)00630-X. [\[Link\]](#)
- Chen, J., G. Li, J. Yang, W. Rao, H. Lu, W. Balsam, Y. Sun, and J. Ji, 2007: Nd and Sr isotopic characteristics of Chinese deserts: Implications for the provenances of Asian dust. *Geochim. Cosmochim. Acta*, **71**, 3904-3914, doi: 10.1016/j.gca.2007.04.033. [\[Link\]](#)
- Chow, J. C., J. G. Watson, J. E. Houck, L. C. Pritchetta, C. F. Rogers, C. A. Frazier, R. T. Egamia, and B. M. Balla, 1994: A laboratory resuspension chamber to measure fugitive dust size distributions and chemical compositions. *Atmos. Environ.*, **28**, 3463-3481, doi: 10.1016/1352-2310(94)90005-1. [\[Link\]](#)
- Gallet, S., B. Jahn, and M. Torri, 1996: Geochemical characterization of the Luochuan loess-paleosol sequence, China, and paleoclimatic implications. *Chem. Geol.*, **133**, 67-88, doi: 10.1016/S0009-2541(96)00070-8. [\[Link\]](#)
- Godfrey, L. V., 2002: Temporal changes in the lead isotopic composition of red clays: Comparison with ferromanganese crust records. *Chem. Geol.*, **185**, 241-254, doi: 10.1016/S0009-2541(01)00406-5. [\[Link\]](#)
- Jahn, B., S. Gallet, and J. Han, 2001: Geochemistry of the Xining, Xifeng and Jixian sections, Loess Plateau of China: Eolian dust provenance and paleosol evolution during the last 140 ka. *Chem. Geol.*, **178**, 71-94, doi: 10.1016/S0009-2541(00)00430-7. [\[Link\]](#)
- Jones, C. E., A. N. Halliday, D. K. Rea, and R. M. Owen, 2000: Eolian inputs of lead to the North Pacific. *Geochim. Cosmochim. Acta*, **64**, 1405-1416, doi: 10.1016/S0016-7037(99)00439-1. [\[Link\]](#)
- Klemm, V., B. Reynolds, M. Frank, T. Pettke, and A. N. Halliday, 2007: Cenozoic changes in atmospheric lead recorded in central Pacific ferromanganese crusts. *Earth Planet. Sci. Lett.*, **253**, 57-66, doi: 10.1016/j.epsl.2006.10.018. [\[Link\]](#)
- Li, F., 2007: Distribution characteristics of lead isotope in dust source areas and its trace significance in north of China. *J. Desert Res.*, **25**, 738-744. (in Chinese)
- Liu, T. S., 1985: Loess and Environment. China Ocean Press, Beijing.
- Pettke, T., A. N. Halliday, C. M. Hall, and D. K. Rea, 2000: Dust production and deposition in Asia and the North Pacific Ocean over the past 12 Myr. *Earth Planet. Sci. Lett.*, **178**, 397-413, doi: 10.1016/S0012-821X(00)00083-2. [\[Link\]](#)
- Porter, S. C., 2001: Chinese loess record of monsoon climate during the last glacial-interglacial cycle. *Earth-Sci. Rev.*, **54**, 115-128, doi: 10.1016/S0012-8252(01)00043-5. [\[Link\]](#)
- Porter, S. C. and Z. An, 1995: Correlation between climate events in the North Atlantic and China during the last glaciation. *Nature*, **375**, 305-308, doi: 10.1038/375305a0. [\[Link\]](#)
- Stancin, A. M., J. D. Gleason, D. K. Rea, R. M. Owen, T. C. Moore Jr., J. D. Blum, and S. A. Hovan, 2006: Radiogenic isotopic mapping of late Cenozoic eolian and hemipelagic sediment distribution in the east-central Pacific. *Earth Planet. Sci. Lett.*, **248**, 840-850, doi: 10.1016/j.epsl.2006.06.038. [\[Link\]](#)
- Sun, J., 2002: Provenance of loess material and formation of loess deposits on the Chinese Loess Plateau. *Earth Planet. Sci. Lett.*, **203**, 845-859, doi: 10.1016/S0012-821X(02)00921-4. [\[Link\]](#)
- Sun, J. and X. Zhu, 2010: Temporal variations in Pb isotopes and trace element concentrations within Chinese eolian deposits during the past 8 Ma: Implications for

- provenance change. *Earth Planet. Sci. Lett.*, **290**, 438-447, doi: 10.1016/j.epsl.2010.01.001. [[Link](#)]
- Sun, Y. and Z. An, 2002: History and variability of Asian interior aridity recorded by eolian flux in the Chinese Loess Plateau during the past 7 Ma. *Sci. China Ser. D: Earth Sci.*, **45**, 420-429, doi: 10.1360/02yd9044. [[Link](#)]
- Sun, Y., R. Tada, J. Chen, Q. Liu, S. Toyoda, A. Tani, J. Ji, and Y. Isozaki, 2008: Tracing the provenance of fine-grained dust deposited on the central Chinese Loess Plateau. *Geophys. Res. Lett.*, **35**, L01804, doi: 10.1029/2007GL031672. [[Link](#)]
- Veysseyre, A. M., A. F. Böllhofer, K. J. R. Rosman, C. P. Ferrari, and C. F. Boutron, 2001: Tracing the origin of pollution in French Alpine snow and aerosols using lead isotopic ratios. *Environ. Sci. Technol.*, **35**, 4463-4469, doi: 10.1021/es0105717. [[Link](#)]
- Walder, A. J. and N. Furuta, 1993: High-precision lead isotope ratio measurement by inductively coupled plasma multiple collector mass spectrometry. *Anal. Sci.*, **9**, 675-680.
- Zhang, X. Y., R. Arimoto, and Z. S. An, 1997: Dust emission from Chinese desert sources linked to variations in atmospheric circulation. *J. Geophys. Res.*, **102**, 28041-28047, doi: 10.1029/97JD02300. [[Link](#)]
- Zhu, B., 1995: The mapping of geochemical provinces in China based on Pb isotopes. *J. Geochem. Explor.*, **55**, 171-181, doi: 10.1016/0375-6742(95)00011-9. [[Link](#)]